Inorganic Chemistry

Article

pubs.acs.org/IC

Coordination-Induced Condensation of $[Ta_6O_{19}]^{8-}$: Synthesis and Structure of $[\{(C_6H_6)Ru\}_2Ta_6O_{19}]^{4-}$ and $[\{(C_6H_6)RuTa_6O_{18}\}_2(\mu\text{-}O)]^{10-}$

P. A. Abramov,[†,‡] M. N. Sokolov,*[,†,‡] S. Floquet,[§] M. Haouas,[§] F. Taulelle,[§] E. Cadot,[§] E. V. Peresypkina,[†,‡] A. V. Virovets,[†,‡] C. Vicent,[∥] N. B. Kompankov,[†] A. A. Zhdanov,[†,‡] O. V. Shuvaeva,[†] and V. P. Fedin[†,‡]

[†]Nikolaev Institute of Inorganic Chemistry SB RAS, 3, Akad. Lavrentiev Avenue, Novosibirsk 630090, Russia

[‡]Novosibirsk State University, Novosibirsk 630090, Russia

[§]Institut Lavoisier de Versailles, UMR 8180, University of Versailles Saint-Quentin en Yvelines, 45 Avenue des Etats-Unis, 78035 Versailles, France

[∥]Serveis Centrals d'Instrumentació Científica, Universitat Jaume I, Av. Sos Baynat s/n, 12071 Castelló, Spain

Supporting Information

ABSTRACT: Reaction of $[(C_6H_6)RuCl_2]_2$ and $Na_8[Ta_6O_{19}]$ gives two new hybrid organometallic POM complexes, $Na_{10}[\{(C_6H_6)RuTa_6O_{18}\}_2(\mu\text{-}O)]\cdot 39.4H_2O$ (**Na_{10}-1**) and $Na_4(trans\text{-}[\{(C_6H_6)Ru\}_2Ta_6O_{19}]\cdot 20H_2O$ (**Na_4-2**). In both cases the half-sandwich fragments $\{(C_6H_6)Ru\}^{2+}$ are coordinated as additional vertices to the $\{Ta_3(\mu_2\text{-}O)_3\}$ triangles of the hexatantalate. According to NMR and ESI-MS data, the dimeric complex $[\{(C_6H_6)RuTa_6O_{18}\}_2(\mu\text{-}O)]^{10-}$ dissociates in water with the formation of monomeric $[(C_6H_6)RuTa_6O_{19}]^{6-}$ species (**1a**). X-ray structural characterization and aqueous speciation of the complexes by ^{13}C, ^{1}H, and DOSY NMR; ESI-MS; and capillary electrophoresis (CE) have been carried out.

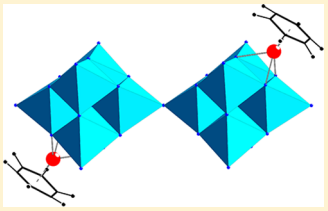

INTRODUCTION

The solution chemistry of polyoxotantalates belongs to the least studied area of the polyoxometalate (POM) chemistry. The key species in this chemistry is the very stable (under basic conditions) anion $[Ta_6O_{19}]^{8-}$. Hexatantalates of various cationic compositions $A_xB_y[Ta_6O_{19}]\cdot nH_2O$ (A and B = Na, K, Rb, Cs, x = 7, 8; y = 0, 1; n = 0, 4, 14, 16) are known,[1,2] with the recent additions of $Na_8[Ta_6O_{19}]\cdot 24.5H_2O$[3] and $(NBu_4)_6[H_2Ta_6O_{19}]\cdot 10H_2O$.[4] A decade ago, Pope et al. used $[M_6O_{19}]^{8-}$ (M = Nb, Ta) as robust inorganic tridentate ligands in reactions with $[Mn(CO)_3(CH_3CN)_3]ClO_4$ or $[Re(CO)_5Br]$, which gave *trans*-$[(M'(CO)_3)_2M_6O_{19}]^{6-}$.[5] In 2007, Proust et al. reported the syntheses of various compounds combining the complex $\{(p\text{-}cym)Ru\}^{2+}$ (p-cym = *para*-cymene) and the anion $[Nb_6O_{19}]^{8-}$ with Ru/POM stoichiometries ranging from 1:1 to 4:1.[6] Complexes of POM with $\{(arene)Ru\}^{2+}$ can be used for construction of hybrid POM−organometallic materials and can find applications in catalysis, as, for example, in the racemization of secondary alcohols catalyzed by $[\{(arene)Ru\}_4M_4O_{16}]$ (M = Mo, W),[7] or in oxidations of *n*-hexadecane and *p*-xylene.[8]

The half-sandwich fragment $\{(arene)Ru\}^{2+}$ belongs to the family of the isolobal fragments d^0-*fac*-$\{MO_2(OR)\}^+$ and d^6-*fac*-$\{ML_3\}$ (ML_3 = $M(CO)_3$ (M = Mn, Re), (arene)Ru, CpRh), among which Ru(II) monoarene complexes represent one of the most popular building blocks for grafting of a noble metal (Ru) to a POM.[9] It coordinates to $[V_6O_{19}]^{8-}$ and stabilizes it by coordination;[10] with molybdate, it produces $[\{(arene)Ru\}_4Mo_4O_{16}]$ (arene = C_6Me_6, toluene, mesitylene, or durene).[11,12] A mixture of the $[(p\text{-}cym)RuCl_2]_2$ and $[Cp^*RhCl_2]_2$ reacts with Na_2MoO_4 to give heterotrimetallic complexes $[\{(p\text{-}cym)Ru\}(Cp^*Rh)_3Mo_4O_{16}]$ and $[\{(p\text{-}cym)Ru\}_2(Cp^*Rh)_2Mo_4O_{16}]$.[13] Other complexes, such as $[\{(arene)Ru\}_2Mo_6O_{20}(OMe)_2]^{2-}$ (arene = C_6Me_6, toluene), $[\{(p\text{-}cym)Ru\}Mo_2O_4(MeC(CH_2O)_3)_2]$, and $[\{(C_6Me_6)Ru\}_2Mo_6O_{18}(MeC(CH_2O)_3)_2]^{2-}$ were isolated by varying the reaction conditions and arenes.[14] The monolacunary Lindqvist anion $[Mo_5O_{18}]^{6-}$ supports three $\{(C_6Me_6)Ru\}^{2+}$ groups in the complex $[\{(C_6Me_6)Ru\}_2\{(C_6Me_6)Ru(H_2O)\}Mo_5O_{18}]$.[11] This complex was obtained by reaction of $[(C_6Me_6)RuCl_2]_2$ with Na_2MoO_4 or with $(Bu_4N)_2[Mo_2O_7]$. It was tested, together with $[\{(C_6Me_6)Ru\}_2\{(C_6Me_6)Ru(H_2O)\}Mo_5O_{18}]$, $[(C_6Me_6)RuCl_2]_2$, and $[(p\text{-}cym)RuCl_2]_2$, in hydroxylation of adamantane with 2,6-dichloropyridine *N*-oxide. Selective conversions up to 94% based on the substrate were achieved with this catalyst. A high valence Ru═O complex generated in situ was suggested as the catalytically active species.[15] Another POM with double-cubane structure, $[\{(p\text{-}cym)Ru\}_4W_2O_{10}]$, was obtained as a byproduct in the preparation of $[\{(p\text{-}cym)Ru\}_4W_4O_{16}]$.[11,16] The same reactions, carried out in water instead of acetonitrile, resulted in the formation of $[\{(p\text{-}cym)Ru\}_2(\mu\text{-}OH)_3]_2[\{(p\text{-}cym)Ru\}_2\{(p\text{-}cym)Ru(H_2O)\}_2W_8O_{28}(OH)_2]$ with polyanions made of two cubes joined by two *cis*-$\{WO_2\}^{2+}$ groups;[16] moreover, $Na_2[W_8O_{30}\{(C_6H_6)Ru\}_2\{(C_6H_6)Ru(H_2O)\}_2]\cdot 16H_2O$ was recently synthesized.[17]

Received: July 17, 2014
Published: December 3, 2014

   dx.doi.org/10.1021/ic501622t | *Inorg. Chem.* 2014, 53, 12791−12798

Grafting of $\{(C_6H_6)Ru\}^{2+}$ complex on the Dawson-type anion $[P_2Nb_3W_{15}O_{62}]^{9-}$ yields $[\{(C_6H_6)Ru\}\text{-}P_2Nb_3W_{15}O_{62}]^{7-}$.[18] The organometallic moiety attaches regiospecifically to the $\{Nb_3O_9\}$ group.[19,20] This complex catalyzes oxygenation of cyclohexene with O_2 into a mixture of 2-cyclohexenone and 2-cyclohexen-1-ol.[21] $\{(C_6H_6)Ru\}^{2+}$ can be grafted on $[1,2,3\text{-}\alpha\text{-}P_2V_3W_{15}O_{62}]^{9-}$ either over one of the three vanadium octahedra, with bonds to two bridging and one terminal oxygen, or over the central site between vanadium octahedra, with bonds to three bridging oxygens, depending on the reaction conditions (solvent and temperature).[22]

To the best of our knowledge, no data about coordination of $\{(C_6H_6)Ru\}^{2+}$ to $[Ta_6O_{19}]^{8-}$ could be found. In this work, we report our studies on the reactivity $[(C_6H_6)RuCl_2]_2$ with the hexatantalate $[Ta_6O_{19}]^{8-}$.

EXPERIMENTAL SECTION

$Na_8[Ta_6O_{19}]\cdot 24.5H_2O$ was synthesized by reacting Ta_2O_5 with NaOH melt followed by extraction with water.[3] $[(C_6H_6)RuCl_2]_2$ was prepared as described in the literature.[23] Other reagents were of commercial quality and used as purchased.

TG experiments were done at NETZSCH TG 209 F1 device in Al_2O_3 crucible at 22 to 300 °C with 10 °C gradient. IR spectra (4000–400 cm^{-1}) were recorded on an IFS-85 Bruker spectrometer. Elemental analyses were carried out at the analytical service of the Institute of Inorganic Chemistry (Novosibirsk). EDX measurements were performed on a JEOL JSM 5800LV apparatus. Capillary electrophoresis was carried out with Agilent G1600AX equipped with internal UV–vis detector. Typical conditions follow: fused-silica capillary 50 μm i.d. × 75 sm; sample buffer 7.5×10^{-3} M borate (pH 9.18); running buffer 7.5×10^{-2} M borate (pH 9.18); hydrodynamic injection 300 mbar × s; applied voltage −30 kV; direct UV-detection mode at 254 nm.

Electrospray ionization (ESI) mass spectra were recorded on a QTOF Premier (quadrupole-T-wave-time-of-flight) instrument. The temperature of the source block was set to 100 °C, and the desolvation temperature to 200 °C. A capillary voltage of 3.3 kV was used in the negative scan mode, and the cone voltage was set to 10 V to control the extent of fragmentation of the identified species. Mass calibration was performed using a solution of sodium iodide in isopropanol:water (50:50) from m/z 50 to 3000. Sample solutions ca. 5×10^{-5} M in water were injected via syringe pump directly connected to the ESI source at a flow rate of 10 μL/min. The observed isotopic pattern of each compound perfectly matched the theoretical isotope pattern calculated from their elemental composition using the MassLynx 4.1 program. The intrinsic stability of compound **Na_4-2** was studied by preparing 1×10^{-4} M solutions of **2** and adding increasing amounts of concentrated 1 M NaOH and 1 M HCl (in order to minimize the volume change) to reach the desired pH value. Sample solutions were filtered through 0.2 μm filters prior to introduction in the ESI mass spectrometer.

NMR. ^{1}H and ^{13}C NMR spectra were recorded on a Bruker Avance 500 spectrometer with inner references in D_2O at room temperature. Translational diffusion measurements were performed using Bruker's "ledbpgs2s" stimulated echo DOSY pulse sequence including bipolar and spoil gradients. Apparent diffusion coefficients were obtained using an adapted algorithm based on the inverse Laplace transform and maximum entropy.

X-ray Crystallography. Crystallographic data and refinement details are given in Supporting Information Table S1. The diffraction data were collected on a Bruker X8Apex CCD diffractometer with Mo Kα radiation (λ = 0.710 73 Å) by doing φ and ω scans of narrow (0.5°) frames. Structures of **Na_{10}-1** and **Na_4-2** were solved by direct methods and refined by full-matrix least-squares treatment against $|F^2|$ in anisotropic approximation with SHELXTL programs set.[24] Absorption corrections were applied empirically with SADABS program.[25] The structure of **Na_{10}-1** was seriously disordered. The dimeric anion $[\{Ta_6O_{18}\}_2(\mu\text{-}O)]^{10-}$ is ordered and occupies special position 4*b* of the *Cmca* (*Cmce* in modern notation) space group with the site symmetry C_{2h}. The $\{(C_6H_6)Ru\}^{2+}$ group lies on the mirror plane and is disordered over two positions with relative occupancy refined to 0.6/0.4. The cationic part and solvent water molecules are disordered, so that the position of one of the Na^+ overlaps with that of a $\{(C_6H_6)Ru\}^{2+}$ group (Figure S7 in Supporting Information). The positions of disordered atoms were found on residual density maps and refined isotropically (except for Ru atoms). All non-hydrogen atoms in **Na_4-2** were refined anisotropically. Hydrogen atoms of benzene rings in both **Na_{10}-1** and **Na_4-2** were set geometrically and refined riding on a pivot carbon atom. Hydrogen atoms of water molecules were not located. Further details may be obtained from the Cambridge Crystallographic Data Center on quoting the depository numbers CCDC 1009646–1009647. Copies of this information may be obtained free of charge from http://www.ccdc.cam.ac.uk.

Crystal packing motifs were analyzed using TOPOS 4.0 Professional program set.[26]

*Synthesis of $Na_{10}[\{(C_6H_6)RuTa_6O_{18}\}_2(\mu\text{-}O)]\cdot 39.4H_2O$ (**Na_{10}-1**).* $Na_8[Ta_6O_{19}]\cdot 24.5H_2O$ (0.050 g, 0.025 mmol) was dissolved in 2 mL of H_2O (pH = 11.5) under stirring and heating at 80 °C. To a clear solution, 0.007 g (0.014 mmol) of $[(C_6H_6)RuCl_2]_2$ was added. The reaction mixture was kept under stirring at 80 °C for 8 h, then a small amount of precipitate was filtered off, and the resulting yellow solution (the final pH was 8.4) was left in air for slow evaporation at room temperature. In 2 days yellow plates of **Na_{10}-1** were collected. Yield 80%.

IR (KBr, cm^{-1}): 3379(br), 2208(br), 1655(s), 1437(m), 852(s), 774(s), 682(s), 544(s), 473(s).

^{1}H NMR (**1a**) (D_2O + H_2O, r.t., δ, ppm): 5.85. ^{13}C NMR (D_2O + H_2O, r.t., δ, ppm): 81.4.

Anal. for $C_{12}H_{90.8}Na_{10}O_{76.4}Ru_2Ta_{12}$ (**Na_{10}-1**) Calcd C, H (%): 3.5; 2.3. Found C, H (%): 3.2, 2.3. EDX ratios found (expected): Ta/Ru = 5.86 (6.00).

TGA: 16.2% weight loss between room temperature and 280 °C corresponding to 34 water molecules (calculated: 16.29%)

*Synthesis of $Na_4(trans\text{-}[\{(C_6H_6)Ru\}_2Ta_6O_{19}])\cdot 20H_2O$ (**Na_4-2**).* $Na_8[Ta_6O_{19}]\cdot 24.5H_2O$ (0.15 g, 0.074 mmol) was dissolved in 2 mL of H_2O, followed by addition of 0.04 g (0.08 mmol) of $[(C_6H_6)\text{-}RuCl_2]_2$. The mixture was heated under stirring at 80 °C for 8 h, then a small amount of precipitate was filtered off, and the resulting yellow solution (final pH was 7.6) was left in air for slow evaporation at room temperature. In 2 days yellow crystals of **Na_4-2** were collected. Yield 0.1 g (80%). The crude product can be precipitated from aqueous solution by addition of EtOH.

IR (KBr, cm^{-1}): 3389(w), 3079(s), 2959(s), 2875(m), 2254(br), 1635(s), 1474(w), 1435(w), 874(s), 771(s), 707(s), 621(s), 544(s).

^{1}H NMR (D_2O, r.t., δ, ppm): 5.93. ^{13}C NMR(D_2O + H_2O, r.t., δ, ppm): 81.8.

Analysis for $C_{12}H_{46}Na_4O_{39}Ru_2Ta_6$, Calcd: C, 6.56; H, 2.11; Na, 4.19%. Found: C, 6.95, H, 2.15; Na, 4.03%. EDX atomic ratio found (expected): Ta/Ru = 3.02 (3.00). TGA: 16.4% weight loss between room temperature and 170 °C corresponding to 20 water molecules (calculated: 16.36%)

RESULTS AND DISCUSSION

Synthesis and Reactivity. Freshly prepared solution of $Na_8[Ta_6O_{19}]\cdot 24.5H_2O$ in water (50 mg in 2 mL) has pH 11.5 due to proton transfer from H_2O to highly basic $[Ta_6O_{19}]^{8-}$. Coordination of $\{(C_6H_6)Ru\}^{2+}$ to $[Ta_6O_{19}]^{8-}$ reduces the high negative charge of hexatantalate and decreases the degree of protonation, thus diminishing the pH value as the complexation proceeds. We have found that heating a mixture of $Na_8[Ta_6O_{19}]\cdot 24.5H_2O$ and $[(C_6H_6)RuCl_2]_2$ in water (POM/Ru ratio 1:1) leads to a yellow solution which corresponds to the formation of the single-capped $[(C_6H_6)RuTa_6O_{19}]^{6-}$ (**$1a^{6-}$**) anion. The progress of the reaction can be monitored by electrospray ionization mass spectrometry (ESI-MS) operating in the negative scan mode. Figure 1a displays the ESI(−) mass

dx.doi.org/10.1021/ic501622t | Inorg. Chem. 2014, 53, 12791–12798

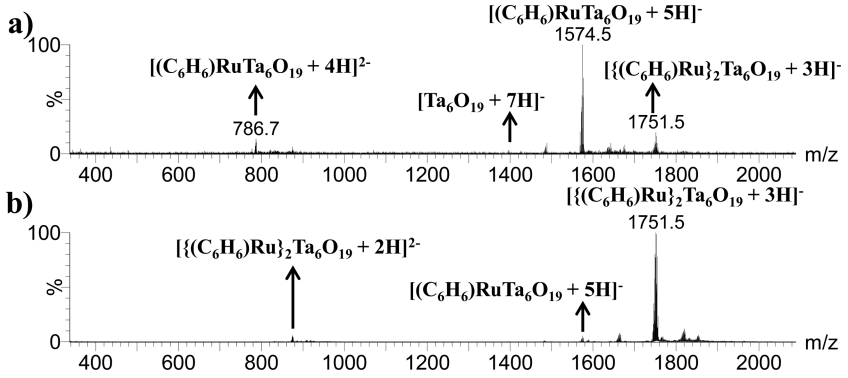

Figure 1. ESI(−) mass spectra of aqueous solutions recorded at U_c = 10 V of the products of reaction between $Na_8[Ta_6O_{19}]\cdot 24.5H_2O$ and $[(C_6H_6)RuCl_2]_2$ in water with POM/Ru ratio 1:1 (a) and 1:2 (b).

spectrum of aqueous solutions of pure **1a**$^{6-}$ recorded under gentle conditions, U_c = 10 V, and a comparison between experimental and simulated isotopic patterns of the identified species is shown in Supporting Information Figure S1.

The ESI(−) mass spectrum features the $[(C_6H_6)RuTa_6O_{19} + 5H]^-$ anion (m/z 1574.5) as the base peak accompanied by a minor signal due to the doubly charged $[(C_6H_6)RuTa_6O_{19} + 4H]^{2-}$ species (m/z 786.7) that corresponds to a lesser extent of protonation. A minor peak at m/z 1751.5 was also observed, which corresponds to the $[\{(C_6H_6)Ru\}_2Ta_6O_{19} + 3H]^-$ anion with two capping $\{RuC_6H_6\}^{2+}$ units. The presence of the $[Ta_6O_{19}]^{8-}$ species was also revealed by ESI-MS as $[Ta_6O_{19} + 7H]^-$ species at m/z 1396.6. Species derived from both the doubly substituted $[\{(C_6H_6)Ru\}_2Ta_6O_{19}]^{4-}$ and $[Ta_6O_{19}]^{8-}$ anions were repeatedly observed by ESI-MS even in the solutions of purified samples of **Na_{10}-1**, suggesting a dynamic equilibrium between both species in solution. Slow evaporation of this solution in air gives yellow plates of **Na_{10}-1**, characterized by X-ray analysis. It contains unexpected $[\{(C_6H_6)RuTa_6O_{18}\}_2(\mu\text{-O})]^{10-}$ anions (Figure 2) built of two fragments $\{(C_6H_6)RuTa_6O_{18}\}$ combined together via a common μ_2-O bridge.

The formation of $[\{(C_6H_6)RuTa_6O_{18}\}_2(\mu\text{-O})]^{10-}$ can be viewed as coordination-induced condensation of two hexatantalate ions as depicted in equilibrium 1:

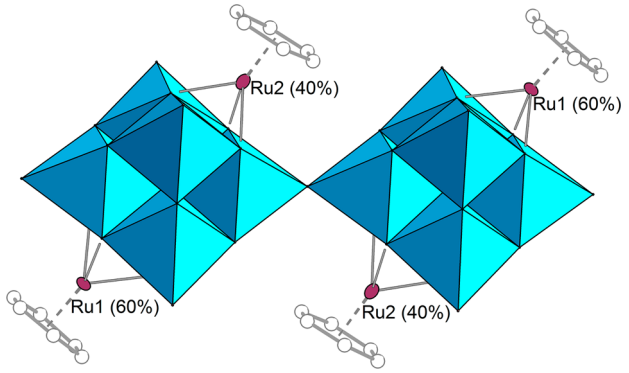

Figure 2. Structure of $[\{(C_6H_6)RuTa_6O_{18}\}_2(\mu\text{-O})]^{10-}$ anion in **Na_{10}-1**, hydrogen atoms of arene rings are not shown for clarity. Both disordered positions of $(C_6H_6)Ru$ fragments are shown together with relative occupancies.

$$[\{(C_6H_6)Ru\}Ta_6O_{19}]^{6-} + H_2O = [\{(C_6H_6)Ru\}Ta_6O_{19}H]^{5-} + OH^-$$

$$2[\{(C_6H_6)Ru\}Ta_6O_{19}H]^{5-} = [\{(C_6H_6)RuTa_6O_{18}\}_2(\mu\text{-O})]^{10-} + H_2O \quad (1)$$

Such condensation is not observed in the case of free, noncoordinated hexatantalate. Perhaps the reduced charge of the 1:1 complex $[\{(C_6H_6)Ru\}Ta_6O_{19}]^{6-}$ facilitates interaction between two negatively charged species. Moreover, coordination of electron-accepting fragment $\{(C_6H_6)Ru\}^{2+}$ can affect electronic density on the oxygen atoms of the POM part. It is worth noting that ESI(−) mass analysis of redissolved crystals of **Na_{10}-1** in water invariably revealed only the presence of the monomeric **1a**$^{6-}$ anion, without any indications of the presence of the dimer, thus indicating that the dimerization depicted in eq 1 is a reversible process on going from the solution to the solid state and vice versa.

Decreasing the POM/Ru ratio to 1:2 leads, under the same conditions, to the expected complex $[\{(C_6H_6)Ru\}_2Ta_6O_{19}]^{4-}$ (**2**) isolated as Na_4(*trans*-$[\{(C_6H_6)Ru\}_2Ta_6O_{19}]\cdot 20H_2O$ (**Na_4-2**). The ESI(−) mass spectrum is illustrated in Figure 1b and, like **1a**$^{6-}$, displays the $[\{(C_6H_6)Ru\}_2Ta_6O_{19} + 3H]^-$ anion (m/z 1751.5) as the base peak, accompanied by a minor signal from the doubly charged $[\{(C_6H_6)Ru\}_2Ta_6O_{19} + 2H]^{2-}$ dianion (m/z 875.3). The singly coordinated **1a**$^{6-}$ species (observed as a minor species at m/z 1574.5 in the ESI(−) mass spectrum) coexists with the $[\{(C_6H_6)Ru\}_2Ta_6O_{19}]^{4-}$ anion, once again suggesting a plausible dynamic equilibrium between both species. ESI(+) mass spectrum (see Supporting Information Figure S8) revealed the presence of the $[(C_6H_6)_2Ru_2(OH)_3]^+$ cation as the dominant peak.

Thus, the formation of $\{(C_6H_6)Ru\}^{2+}/[Ta_6O_{19}]^{8-}$ complexes in solution and solid state can be illustrated by Scheme 1.

The ^{13}C NMR spectrum of the solution after separation of **Na_4-2** shows one intense signal at 77.8 ppm, attributable to $[(C_6H_6)_2Ru_2(\mu\text{-OH})_3]^+$, together with a group of very weak signals at 78.6, 78.9, and 79.7 ppm assigned to different $[(C_6H_6)_2Ru_2(\mu\text{-OH})_xCl_{3-x}]^+$ species. From these solutions only $[(C_6H_6)_2Ru_2(\mu\text{-OH})_3]Cl\cdot 3H_2O$[27] was isolated.

IR spectrum of **Na_{10}-1** shows strong $[Ta_6O_{19}]^{8-}$-related bands at 852, 682, and 544 cm^{-1}. For comparison, in $Na_8[Ta_6O_{19}]\cdot 24.5H_2O$ these bands are observed at 842, 687, and 532 cm^{-1}.[3] On the basis of treatment given in ref 28, they can be assigned as ν_{as}(Ta−O$_t$), δ_s(Ta−O$_{br}$), and δ_{as}(Ta−O$_{br}$), respectively. The band at 774 cm^{-1} can be assigned to the linear

dx.doi.org/10.1021/ic501622t | *Inorg. Chem.* 2014, 53, 12791−12798

Scheme 1. Formation of 1:1 and 1:2 Complexes from Hexatantalate and $[(C_6H_6)RuCl_2]_2$

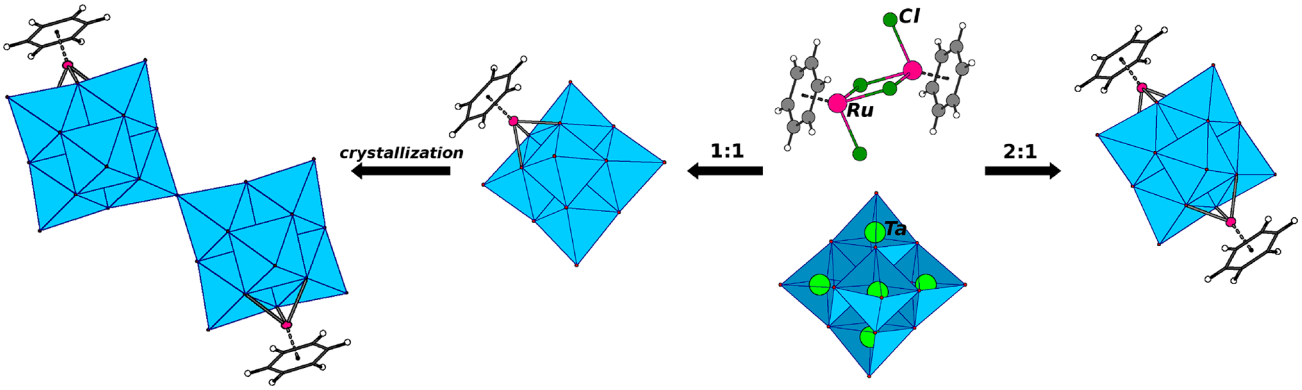

Scheme 2. Three Types of Possible Isomers of $[(Ta_6O_{18})_2O]^{10-}$ Anion in a Crystal Structure of Na_{10}-1

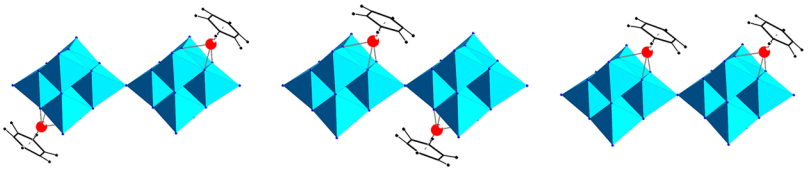

Ta−O−Ta bridge between two $\{Ta_6O_{18}\}$ units. It can be compared with δ(Ti−O−Ti) value of 716 cm^{-1} reported for $[(TiMo_5O_{18})_2(\mu\text{-O})]^{6-}$.[29]

The dimeric $[(Ta_6O_{18})_2O]^{10-}$ anion **1** in the crystal structure of **Na_{10}-1** lies in the center of symmetry of the space group *Cmca*. As a result there is only one crystallographically independent $\{Ta_6O_{18}\}$ unit that coordinates $\{(C_6H_6)Ru\}^{2+}$ fragment. The latter is disordered over 2 positions (Ru1 and Ru2, Supporting Information Figure S7) with relative occupancies refined as 0.6/0.4. In order to rationalize this disorder possible ways of coordination of $\{(C_6H_6)Ru\}^{2+}$ fragment to $\{Ta_6O_{18}\}$ units have to be considered. Each unit has 8 equally available positions for the coordination of a $\{(C_6H_6)Ru\}^{2+}$ fragment, corresponding to the triangular faces of a Ta_6 octahedron. Taking into account free rotation around the μ-O bridge and assuming that each $\{Ta_6O_{18}\}$ unit bears only one $\{(C_6H_6)Ru\}^{2+}$ fragment, the number of possible positions reduces to two in each of $\{Ta_6O_{18}\}$ unit, and only three possible isomers, A (*trans*−*trans*-), B (*cis*−*cis*-), and C (*cis*−*trans*-), can occur (Scheme 2).

The simplest model of the disorder assumes an overlap of only two isomers, A and B (Scheme 1), in ratio A/B 0.6/0.40, being in the same crystallographic position. Theoretically, isomer C also can exist in the crystal. Considering that three isomers are statistically distributed (A/B/C = 0.25/0.25/0.50), the relative portions of the isomers, *a*, *b*, and *c*, can be related with the occupancy factors of Ru1 and Ru2, s_1 and s_2, as $a + c/2 = s_1$, $b + c/2 = s_2$, $s_1 + s_2 = 1$. Therefore, if we assume the presence of C isomer, the A/B/C ratio cannot be calculated from the diffraction data.

According to the Cambridge Structural Database (CSD, V.5.34[30]), the $\{M_6O_{18}\}_2O$ fragment possesses staggered or eclipsed conformation depending on the mutual rotation angle (φ) of the MO_4 squares around M−(μ-O)−M line (Table 1). For example, two polymorphs of $(Bu_4N)_4[(NbW_5O_{18})_2O]$ exist, with different crystal packing features, with either strictly linear Nb−(μ-O)−Nb units, or eclipsed conformation of the $\{NbW_5O_{18}\}$ units similarly to **1**. In contrast, the M−(μ-O)−M angle deviates from 180° in isostructural compounds $(Bu_4N)_4[(TiM_5O_{18})_2O]\cdot 2MeCN$, M = Mo, W.

Table 1. Some Geometrical Characteristics of $[\{M_6O_{18}\}_2O]^{q-}$ Anions According to CSD

formula	anion site symmetry	M−(μ-O), Å	ω(M−(μ-O)−M), deg	φ, deg	ref
$(Bu_4N)_4[(NbW_5O_{18})_2O]$	C_2	1.888	180.0	0.8	31b
$(Bu_4N)_4[(NbW_5O_{18})_2O]$	C_i	1.887	180	0	31a
$(Bu_4N)_4[(TiMo_5O_{18})_2O]\cdot 2MeCN$	C_2	1.801	173.0	−78.6	32
$(Bu_4N)_4[(TiW_5O_{18})_2O]\cdot 2MeCN$	C_2	1.801	173.0	−78.6	29
$Na_{10}[\{(C_6H_6)RuTa_6O_{18}\}_2(\mu\text{-O})]\cdot 39.4H_2O$	C_i	1.898	180	0	1

Equilibrium between hexanuclear and oxo-bridged dodecanuclear species seems to be a general feature of the Lindquist-type $[M_6O_{19}]^{n-}$ anions, if they contain a group 5 or 4 transition metal (Ti, Nb). In the case of the mixed species $[M'M_5O_{19}]^{n-}$ it is always the heterometals that participate in the formation of the M′−O−M′ bridge. For solutions of $(Bu_4N)_5[PW_{11}TiO_{40}]$ in CH_3CN, equilibrium between $[PW_{11}TiO_{40}]^{5-}$, protonated $[PW_{11}Ti(OH)O_{40}]^{4-}$, and hydroxo-bridged $[(PTiW_{11}O_{39})_2OH]^{7-}$ was postulated.[33] Finke and Droege reported equilibrium between $[SiW_9Nb_3O_{40}]^{7-}$ and $[Si_2W_{18}Nb_6O_{77}]^{8-}$ with the formation of three Nb−O−Nb bridges between the Keggin-type $\{SiW_9Nb_3\}$ units.[34]

The structure of anion **2** in **Na_4-2** is shown in Figure 3. The anion occupies special position 2*c* of $C_{2/m}$ space group with C_{2h} (2/*m*) point symmetry. Two $\{(C_6H_6)Ru\}^{2+}$ fragments are trans-coordinated to the hexatantalate $[Ta_6O_{19}]^{8-}$ unit via three oxygen atoms of three edge-sharing $\{TaO_6\}$ octahedra. The Ru−O distances in **2** are slightly shorter than in **1** (average of 2.127 vs 2.151 Å).

dx.doi.org/10.1021/ic501622t | *Inorg. Chem.* 2014, 53, 12791−12798

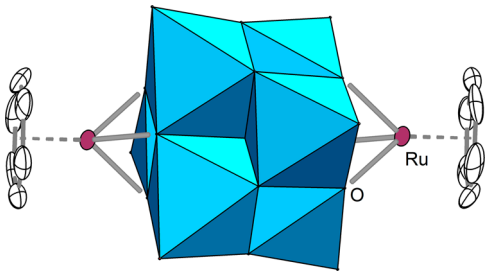

Figure 3. Structure $[\{(C_6H_6)Ru\}_2Ta_6O_{19}]^{4-}$ anion in Na_4-**2**.

Crystal packing of large POM anions in Na_{10}-**1** and Na_4-**2** follows distorted body-centerd (bcc) and face-centerd (fcc) cubic motifs. The sodium cations are surrounded by water molecules and oxygen atoms of POM anions.

Solution Studies. *Aqueous Speciation of* Na_{10}*-1.* $^{13}C\{^1H\}$ and ^1H NMR experiments on aqueous solutions of Na_{10}-**1** were conducted and compared with the data from ESI(−)-MS studies and capillary electrophoresis (CE) experiments. The ^{13}C NMR spectrum of Na_{10}-**1** recorded in D_2O shows one main signal at 81.41 ppm and two small peaks at 81.85 and 81.70 ppm (Figure 4a). Concomitantly, the ^1H NMR spectrum of Na_{10}-**1** displays one main peak at 5.85 (90%) ppm and two minor signals at 5.94 ppm (9%) and 5.99 ppm (≤1%) (Figure 5). In agreement with the ESI(−)-MS data, the major peaks in ^{13}C and in ^1H NMR spectra are attributed to the 1:1 complex $[\{(C_6H_6)Ru\}Ta_6O_{19}]^{6-}$, **1a**, whereas the minor peaks are assigned to the *cis* and *trans* isomers of the 1:2 complex $[\{(C_6H_6)Ru\}_2Ta_6O_{19}]^{4-}$, with the *trans* isomers corresponding probably to the NMR signal at 5.94 ppm, and the *cis* isomer, which is supposed to be less stable than the trans isomer, associated with the signal located at 5.99 ppm. Temperature dependent ^1H NMR spectrum for Na_{10}-**1** shows that at 80 °C the complex is not stable and equilibrates with Na_4-**2**.

The ^1H DOSY NMR technique revealed to be a powerful tool for the determination of the size and the molecular weight

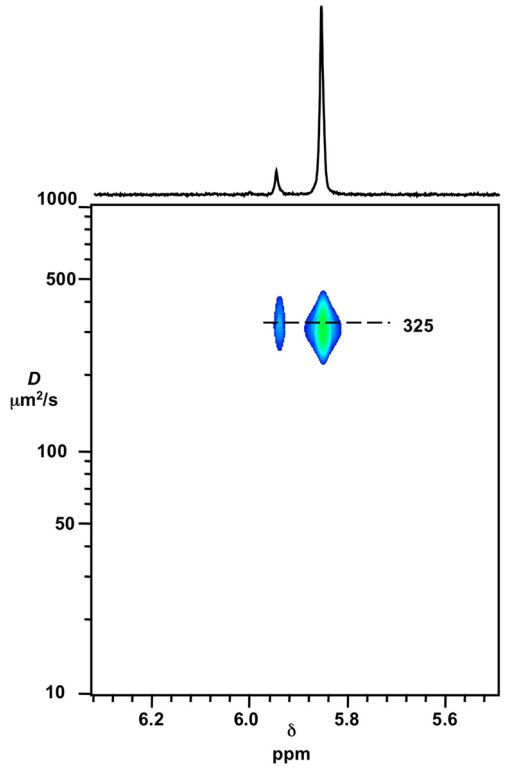

Figure 5. ^1H DOSY NMR spectra of Na_{10}-**1** in D_2O.

of inorganic clusters in aqueous medium.[35] The ^1H DOSY NMR experiment performed on this sample in D_2O (see Figure 5) has yielded the self-diffusion coefficients $D = 315 \pm 10$ μm^2 s^{-1} and $D = 325 \pm 10$ μm^2 s^{-1}, respectively, for the signals located at 5.85 and 5.94 ppm, whereas the intensity of the minor peaks at 5.99 ppm was too low for any accurate determination of the D value. Primarily, these very close values indicate that these species possess similar hydrodynamic radii in

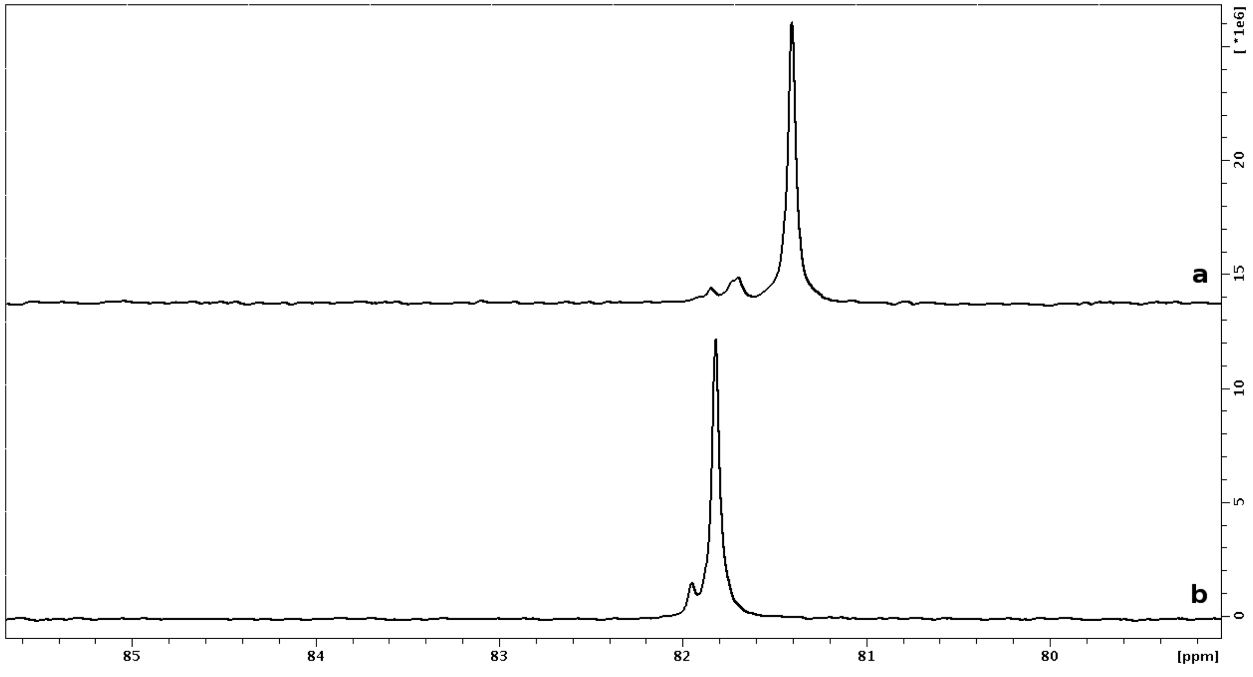

Figure 4. ^{13}C NMR spectra: (a) Na_{10}-**1** in D_2O, (b) Na_4-**2** in D_2O.

dx.doi.org/10.1021/ic501622t | *Inorg. Chem.* 2014, 53, 12791−12798

solution and rule out any participation of the dimeric species. The Stokes–Einstein relation $D = ((kT)/(6\pi\eta R_H))$ (which describes the diffusion coefficient D for spherical objects, where k is the Boltzmann constant, T the temperature taken equal to 300 K in this study, η the solvent viscosity taken equal to that of water at 300 K (1.002 Pa s), and R_H the hydrodynamic radius) applied to these values gives hydrodynamic radii of 6.75–6.96 nm which are compatible with the radii expected for solvated monomeric species $[\{(C_6H_6)Ru\}Ta_6O_{19}]^{6-}$ and $[\{(C_6H_6)Ru\}_2Ta_6O_{19}]^{4-}$ but not with the dimeric anion $[\{(C_6H_6)RuTa_6O_{18}\}_2(\mu\text{-}O)]^{10-}$ which thus confirm our attributions.

Spontaneous dissociation of the dimeric species **Na_{10}-1** in aqueous solution was proved by capillary electrophoresis. The electrophorograms recorded for aqueous solutions of **Na_{10}-1** and **Na_4-2** are shown in Figure 7. Aqueous solutions of **Na_{10}-1**, to which some amount of **Na_4-2** was added as reference, give two well-resolved peaks on the electrophorogram (Figure 7). The second peak in the CE plot corresponded to the cluster **2**, which was confirmed by UV-spectrometry (see Supporting Information Figure S4) and by the standard addition method. The first peak must therefore correspond to the monomeric $[\{(C_6H_6)Ru\}Ta_6O_{19}]^{6-}$ species (or its dominant protonated form), because the signal from the dimer which has larger size and charge should appear after the signal of **2**, with a longer retention time. Thus, both ESI-MS and CE give evidence that in aqueous solutions $[\{(C_6H_6)RuTa_6O_{18}\}_2(\mu\text{-}O)]^{10-}$ dissociates into the monomeric species $[\{(C_6H_6)Ru\}Ta_6O_{19}]^{6-}$.

In summary, the studies performed by the three different techniques are fully consistent with the conclusions (i) that the dimer $[\{(C_6H_6)RuTa_6O_{18}\}_2(\mu\text{-}O)]^{10-}$ does not exist in aqueous solution, being hydrolyzed to afford the $[(C_6H_6)RuTa_6O_{19}]^{6-}$ (**$1a^{6-}$**) as the dominant species, and (ii) that the singly substituted **$1a^{6-}$** anion is in equilibrium with the doubly substituted **2^{4-}** anion $[\{(C_6H_6)Ru\}_2Ta_6O_{19}]^{4-}$ in *trans* and *cis* forms as described by the equilibrium 2 for which we can estimate an equilibrium constant K_2 of around 0.012 on the basis of ^{1}H integration.

$$2[\{(C_6H_6)Ru\}Ta_6O_{19}]^{6-} = [\{(C_6H_6)Ru\}_2Ta_6O_{19}]^{4-} + [Ta_6O_{19}]^{8-} \quad (2)$$

Easy dissociation of the $[\{(C_6H_6)RuTa_6O_{18}\}_2(\mu\text{-}O)]^{10-}$ species is in agreement with reported high reactivity of the M–O–M bridges in related Ti and Nb oxo-bridged Lindquist complexes $[\{TiMo_5O_{18}\}_2(\mu\text{-}O)]^{6-}$ and $[\{NbMo_5O_{18}\}_2(\mu\text{-}O)]^{4-}$. Easy hydrolysis of the latter with the formation of $[NbW_5O_{19}]^{3-}$ takes place in wet CH_3CN. Reaction of $(Bu_4N)_4[(NbW_5O_{18})_2O]$ with alcohols and phenol gives rise to $(Bu_4N)_2[Nb(OR)W_5O_{18}]$ by the cleavage of the Nb–O–Nb linear bridge.[31] In contrast, ^{1}H NMR study of the hydrolysis of $(NBu_4)_3[(OMe)TiW_5O_{18}]$ showed the reaction to be remarkably slow and require long heating times.[29]

*Aqueous Speciation of **Na_4-2**.* The ^{13}C NMR spectrum of **Na_4-2** in D_2O (Figure 4b) exhibits two signals at 81.95 and 81.82 ppm, with the complementary set in the ^{1}H NMR spectrum (Figure 6) at 5.97 (6%) ppm and 5.92 (93%) ppm and 5.85 (≤1%). This pattern most probably corresponds to a mixture of *cis* (6%) and trans (93%) isomers of $[\{(C_6H_6)Ru\}_2Ta_6O_{19}]^{4-}$, similarly to what was observed for $[\{(p\text{-}cym)Ru\}_2Nb_6O_{19}]^{4-}$,[6] and the small peak at 5.85 ppm is to be attributed to the 1:1 complex $[\{(C_6H_6)Ru\}Ta_6O_{19}]^{6-}$. Temperature dependent ^{1}H NMR for **Na_4-2** shows stability of the complex. Aqueous solution of the complex was kept at 80 °C for 2 h, but no changes were detected, indicating that the *cis*/*trans* ratio is not appreciably temperature dependent. The ^{1}H DOSY NMR experiment performed in D_2O gives the self-diffusion coefficients $D = 315 \pm 10$ μm^2 s^{-1} and $D = 325 \pm 10$ μm^2 s^{-1}, respectively, for the signals located at 5.92 and 5.97 ppm, whereas the intensity of the minor peaks at 5.85 ppm is too small for any accurate determination of the D value (Figure 6). These values lead to hydrodynamic radii in the 6.75–6.96 nm range. The latter are identical to that obtained for the previous compound and agree well with our hypotheses: the complex *cis*-$[\{(C_6H_6)Ru\}_2Ta_6O_{19}]^{4-}$ at 5.97 ppm, the complex *trans*-$[\{(C_6H_6)Ru\}_2Ta_6O_{19}]^{4-}$ at 5.92 ppm, and the complex $[\{(C_6H_6)Ru\}Ta_6O_{19}]^{6-}$ at 5.85 ppm.

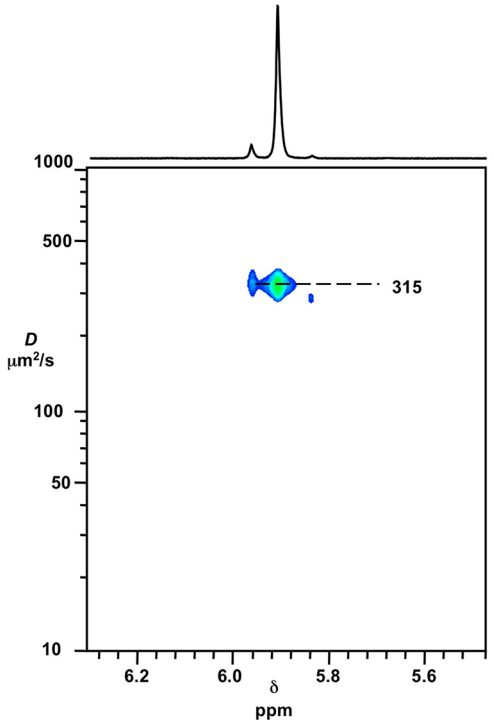

Figure 6. ^{1}H DOSY NMR spectra of **Na_4-2** in D_2O.

These results necessarily imply the equilibria 3 and 4 to occur in solution. The former corresponds to an isomerization process displaced toward the preferred formation of the trans isomer. The latter corresponds to the decoordination of one $\{(C_6H_6)Ru\}^{2+}$ moiety. This hypothesis is supported by the presence of a small broad peak at 5.4 ppm in the ^{1}H NMR spectrum (not shown) attributed to $[(C_6H_6)_2Ru_2(OH)_3]^+$.

$$trans\text{-}[\{(C_6H_6)Ru\}_2Ta_6O_{19}]^{4-} = cis\text{-}[\{(C_6H_6)Ru\}_2Ta_6O_{19}]^{4-} \quad (3)$$

$$2[\{(C_6H_6)Ru\}_2Ta_6O_{19}]^{4-} + 3OH^- + = 2[\{(C_6H_6)Ru\}Ta_6O_{19}]^{6-} + [(C_6H_6)_2Ru_2(\mu\text{-}OH)_3]^+ \quad (4)$$

ESI(−) MS data are consistent with NMR data, since in aqueous solutions of **Na_4-2** doubly and singly substituted **2^{4-}** and **$1a^{6-}$** species coexist, with **2^{4-}** being the dominant species. Additional ESI(−)-MS experiments were conducted in order to evaluate the intrinsic stability of **2^{4-}** over the accessible pH range (see Figure S5, Supporting Information). This technique proved very useful to monitor the composition changes as a

dx.doi.org/10.1021/ic501622t | Inorg. Chem. 2014, 53, 12791–12798

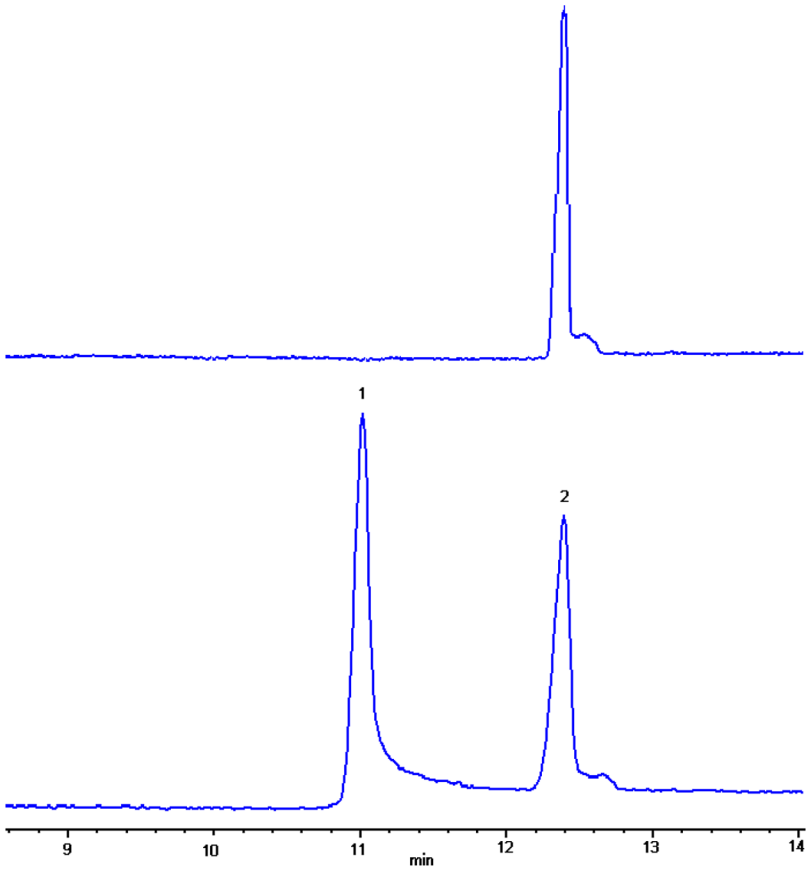

Figure 7. Electrophorogram of complex $\mathbf{Na_4}$-**2** (up). The electrophorogram of complex $\mathbf{Na_{10}}$-**1** solution with addition of complex $\mathbf{Na_4}$-**2** as reference (down). Fused-silica capillary 50 μm i.d. × 75 sm; sample buffer 7.5 × 10^{-3} M borate (pH 9.18); running buffer 7.5 × 10^{-2} M borate (pH 9.18).

function of pH, e.g., in the Mn/Nb POM chemistry by Casey's group.[36] At pH > 5, aqueous solutions were quite stable, and the dominant peaks in the ESI(−) mass spectra were only those derived from $\mathbf{2}^{4-}$. Thus, coordination of the $\{(C_6H_6)Ru\}^{2+}$ moiety increases the stability of the hexatantalate unit beyond the alkaline pH range. We also observed a strong ion suppression as the pH was increased with NaOH. For example, at pH 13, doubly charged peaks formulated as $[\{(C_6H_6)Ru\}_2Ta_6O_{19} + 2cat]^{2-}$ (where "cat" stands indiscriminately for H^+ or Na^+) were observed (see Figure S5, Supporting Information) with significantly reduced ion abundances with respect to aqueous solutions of $\mathbf{2}^{4-}$ in the absence of NaOH. Below pH 5 using HCl, we observed complete disappearance of the Ta/Ru POM species, and the ESI(−) and ESI(+) mass spectra were dominated by adducts of general formula $[Na_{(x-1)}Cl_x]^-$ and $[Na_xCl_{(x-1)}]^-$, respectively. Ru-containing species formulated as $[(C_6H_6)RuCl_3 + n\mathrm{NaCl}]^-$ as well as the $[(C_6H_6)_2Ru_2Cl_5]^-$ anions were also observed, thus indicating that the assembly dismantled leaving only mono- and dinuclear Ru species in solution. Ta-containing species were not detected at all because of precipitation of insoluble Ta(V) hydrated oxide under these conditions.

Under optimal conditions for CE the complex $\mathbf{2}^{4-}$ gives one sharp peak (peak 2 at Figure 7) on electrophorogram, with a small satellite on the rear front. This small peak disappears at pH ≥ 11.5, so we can assume that these two peaks correspond to differently protonated forms of $[\{(C_6H_6)Ru\}_2Ta_6O_{19}]^{4-}$. Investigation of peak purity by the spectral ratio shows that main peak really corresponds to a single species, and UV-spectra are shown in Figure S3 (Supporting Information).

■ ASSOCIATED CONTENT

Ⓢ Supporting Information

ESI(−)-MS data, capillary electrophoresis data, and UV−vis spectrum. Crystallographic data in CIF format. This material is available free of charge via the Internet at http://pubs.acs.org.

■ AUTHOR INFORMATION

Corresponding Author

*E-mail: caesar@niic.nsc.ru.

Notes

The authors declare no competing financial interest.

■ ACKNOWLEDGMENTS

This work was supported by the Centre National de la Recherche Scientifique (CNRS), the project IDEMAT of the French-Siberian Research and Formation Center and the French-Russian LIA CLUSPOM. Authors thank Dr. A. V. Alekseev (XRPD) and Dr. P. E. Plusnin (DTG) for their help with characterization of synthesized polyoxotantalate complexes. The work was partially supported by GC no. 16.740.11.0473 in the framework of the Russian FFP 2009-2013, RFBR grant 13-03-00012, and President of Russian Federation fellowship (PAA).

■ REFERENCES

(1) Hartl, H.; Pickhard, F. *Z. Anorg. Allg. Chem.* **1997**, *623*, 1311.
(2) Hartl, H.; Pickhard, F. *Z. Anorg. Allg. Chem.* **2001**, *627*, 2630.
(3) Abramov, P. A.; Abramova, M. A.; Peresypkina, E. V.; Gushchin, A. L.; Adonin, S. A. *Russ. J. Struct. Chem.* **2011**, *52*, 1012.

(4) Matsumoto, M.; Ozawa, Y.; Yagasaki, A. *Inorg. Chem. Commun.* **2011**, *14*, 115.
(5) Morgenstern, B.; Sander, J.; Huch, V.; Hegetschweiler, K. *Inorg. Chem.* **2001**, *40*, 5307.
(6) Laurencin, D.; Thouvenot, R.; Boubekeur, K.; Proust, A. *Dalton Trans.* **2007**, 1334.
(7) Laurencin, D.; Villanneau, R.; Proust, A.; Brethon, A.; Arends, I. W. C. E.; Sheldon, R. A. *Tetrahedron: Asymmetry* **2007**, *18*, 367.
(8) Bi, L.-H.; Al-Kadamany, G.; Chubarova, E. V.; Dickman, M. H.; Chen, L.; Gopala, D. S.; Richards, R. M.; Keita, B.; Nadjo, L.; Jaensch, H.; Mathys, G.; Kortz, U. *Inorg. Chem.* **2009**, *48*, 10068.
(9) Putaj, P.; Lefebvre, F. *Coord. Chem. Rev.* **2011**, *255*, 1642.
(10) Suss-Fink, G.; Plasseraud, L.; Ferrand, V.; Stanislas, S.; Neels, A.; Stoeckli-Evans, H.; Henry, M.; Laurenczy, G.; Roulet, R. *Polyhedron* **1998**, *17*, 2817.
(11) Artero, V.; Proust, A.; Herson, P.; Gouzerh, P. *Chem.—Eur. J.* **2001**, *7*, 3901.
(12) Laurencin, D.; Fidalgo, E.G.; Villanneau, R.; Villain, F.; Herson, P.; Pacifico, J.; Stoeckli-Evans, H.; Benard, M.; Rohmer, M.-M.; Süss-Fink, G.; Proust, A. *Chem.—Eur. J.* **2004**, *10*, 208.
(13) Plasseraud, L.; Stoeckli-Evans, H.; Suss-Fink, G. *Inorg. Chem. Commun.* **1999**, *2*, 344.
(14) Villanneau, R.; Artero, V.; Laurencin, D.; Herson, P.; Proust, A.; Gouzerh, P. *J. Mol. Struct.* **2003**, *656*, 67.
(15) Bonchio, M.; Scorrano, G.; Toniolo, P.; Proust, A.; Artero, V.; Conte, V. *Adv. Synth. Catal.* **2002**, *344*, 841.
(16) Artero, V.; Proust, A.; Herson, P.; Thouvenot, R.; Gouzerh, P. *Chem. Commun.* **2000**, 883.
(17) Sokolov, M. N.; Kalinina, I. V. Unpublished results.
(18) Weiner, H.; Aiken, J. D.; Finke, R. G. *Inorg. Chem.* **1996**, *35*, 7905.
(19) Edlund, D. J.; Saxton, R. J.; Lyon, D. K.; Finke, R. G. *Organometallics* **1998**, *7*, 1692.
(20) Pohl, M.; Lin, Y.; Weakley, T. J. R.; Nomiya, K.; Kaneko, M.; Weiner, H.; Finke, R. G. *Inorg. Chem.* **1995**, *34*, 767.
(21) Mizuno, N.; Lyon, D. K.; Finke, R. G. *J. Catal.* **1991**, *128*, 84.
(22) Nomiya, K.; Kasahara, Y.; Sado, Y.; Shinohara, A. *Inorg. Chim. Acta* **2007**, *360*, 2313.
(23) Bennett, M. A.; Huang, T.-N.; Matheson, T. W.; Smith, A. K. *Inorg. Synth.* **1982**, *21*, 74.
(24) *SHELXTL (Version 6.12)*; Bruker Advanced X-ray Solutions, Bruker AXS Inc.: Madison, WI, 2004.
(25) *APEX2 (Version 1.08), SAINT (Version 7.03), and SADABS (Version 2.11)*; Bruker Advanced X-ray Solutions, Bruker AXS Inc.: Madison, WI, 2004.
(26) Blatov, V. A. *Newsletter Commission on Crystallographic Computing of IUCr*; 2006; Issue 7, pp 4–38.http://www.iucr.org/iucr-top/comm/ccom/newsletters/.
(27) Kim, T. D.; McNeese, T. J.; Rheingold, A. L. *Inorg. Chem.* **1988**, *27*, 2554.
(28) Mattes, R.; Bierbüsse, H.; Futch, J. *Z. Anorg. Allg. Chem.* **1971**, *385*, 230.
(29) Errington, R. J.; Petkar, S. S.; Middleton, P. S.; McFarlane, W.; Clegg, W.; Coxall, R. A.; Harrington, R. W. *Dalton Trans.* **2007**, 5211.
(30) Allen, F. H. *Acta Crystallogr., Sect. B* **2002**, *58*, 380.
(31) (a) Clegg, W.; Elsegood, M. R. J.; Errington, R. J.; Havelock, J. *Dalton Trans.* **1996**, 681. (b) Lu, Y.-J.; Lalancette, R.; Beer, R. H. *Inorg. Chem.* **1996**, *35*, 2524.
(32) Coyle, L.; Middleton, P. S.; Murphy, C. J.; Clegg, W.; Harrington, R. W.; Errington, R. J. *Dalton Trans.* **2012**, *41*, 971.
(33) Finke, R. G.; Droege, M. W. *J. Am. Chem. Soc.* **1984**, *106*, 7274.
(34) Kholdeeva, O. A.; Maksimov, G. M.; Maksimovskaya, R. I.; Kovaleva, L. A.; Fedotov, M. A.; Grigoriev, V. A.; Hill, C. L. *Inorg. Chem.* **2000**, *39*, 3828.
(35) Floquet, S.; Brun, S.; Lemonnier, J.-F.; Henry, M.; Delsuc, M.-A.; Prigent, Y.; Cadot, E.; Taulelle, F. *J. Am. Chem. Soc.* **2009**, *131*, 17254.
(36) Son, J.-H.; Casey, W. H. *Dalton Trans.* **2013**, *42*, 13339.